DISCRETE SPLINE FILTERS FOR MULTIRESOLUTIONS AND WAVELETS OF l_2*

AKRAM ALDROUBI[†], MURRAY EDEN[†], AND MICHAEL UNSER[†]

Abstract. The authors consider the problem of approximation by B-spline functions, using a norm compatible with the discrete sequence-space l_2 instead of the usual norm L_2. This setting is natural for digital signal/image processing and for numerical analysis. To this end, sampled B-splines are used to define a family of approximation spaces $\mathbf{S}_m^n \subset l_2$. For n odd, $\mathbf{S}_m^n$ is partitioned into sets of multiresolution and wavelet spaces of l_2. It is shown that the least squares approximation in $\mathbf{S}_m^n$ of a sequence $s \in l_2$ is obtained using translation-invariant filters. The authors study the asymptotic properties of these filters and provide the link with Shannon's sampling procedure. Two pyramidal representations of signals are derived and compared: the l_2-optimal and the stepwise l_2-optimal pyramids, the advantage of the latter being that it can be computed by the repetitive application of a single procedure. Finally, a step by step discrete wavelet transform of l_2 is derived that is based on the stepwise optimal representation. As an application, these representations are implemented and compared with the Gaussian/Laplacian pyramids that are widely used in computer vision.

Key words. multiresolution, wavelets, splines, sampling, ideal filter, pyramid

AMS subject classifications. 42C15, 41A15, 94A11, 94A12, 94A15

1. Introduction. Images, signals, and numerical data are usually available to us as a sequence of real or complex numbers. The sequence space l_2 is therefore natural to consider. However, for the purpose of deriving numerical algorithms, it is sometimes desirable to represent an l_2 sequence by an analog function. This is often realized by interpolation techniques [20], [21], [37], [44], [45]. The computations are usually performed numerically on digital computers, and the results are sequences of numbers. Image magnification, reduction, signal coding, and reconstruction are examples [8], [21], [22], [37], [38]. In order to allow for such dual discrete/analog representations, we develop the theory of polynomial spline approximation for discrete sequences. For this purpose, we consider the problem of least squares approximation of discrete functions in the discrete spline spaces:

$$(1) \qquad \mathbf{S}_m^n := \left\{ v \in l_2 : v(k) = \sum_{i \in Z} c(i) b_m^n(k - mi), \quad c \in l_2 \right\},$$

where b_m^n is the sampled B-spline functions of order n (cf. §2.2). It should be noted that any sequence $v \in \mathbf{S}_m^n$ can be obtained by sampling a polynomial spline function of order n (for an extensive treatment of polynomial splines, see [9], [15], [32], [34]). Thus, the approximation of a sequence $s(k)$ in $\mathbf{S}_m^n$ is equivalent to fitting $s(k)$ with a uniformly spaced analog polynomial spline function that minimizes the discrete l_2-norm of the error (cf. Remark 1 in §5.1). For nonuniformly spaced knot points, the latter problem is usually solved by standard matrix techniques [14]. In our case, we treat the uniformly spaced knot points. We show that in this case, the approximation in $\mathbf{S}_m^n$ can be obtained by discrete translation-invariant filtering, as illustrated in Fig. 1. Therefore, this theory is particularly well adapted to signal and image processing. We study the properties of the approximation filters and discuss the theory in light of Shannon's sampling procedure. We then use the results to construct multiresolution

and wavelet spaces for l_2 instead of the usual space L_2 [10], [26], [29], [43]. Other approaches to constructing multiresolution and wavelet spaces of l_2 can be found in [33] (cf. Remark 2 in §5.2).

This paper is organized as follows: In §2, we use discretized B-splines of order n to construct and analyze a family of discrete sequence spaces $\mathbf{S}_m^n$, where n indexes a smoothness constraint and where m is a scale index measuring the coarseness of the space. In §3, we solve the problem of finding the best l_2 approximation to a signal in $\mathbf{S}_m^n$ and show that it can be obtained by a prefiltering followed by a down-sampling, an up-sampling, and an interpolation, as shown in Fig. 1. Both the prefiltering and the interpolation can be carried out by translation-invariant filtering using fast algorithms [41]. In §4, we provide the link between the approximation problem in $\mathbf{S}_m^n$ and the classical Shannon sampling procedure [3], [4], [22], [39]. More specifically, we prove that the frequency response of the prefilters $\overset{\circ}{H}_m^n(f)$ tend to the ideal discrete lowpass filter with periodic support in $\bigcup_{j \in \mathcal{Z}} [j - 1/2m, j + 1/2m]$, and that the discrete spline interpolators $H_m^n(f)$ tend to the ideal lowpass filter with periodic support in $\bigcup_{j \in \mathcal{Z}} [j - 1/2m, j + 1/2m]$ and gain m. Related convergence results for the analog case can be found in [4], [15], [25], [28], [35]. In §5, we use our results to construct and discuss two multiresolution representations of signals: the optimal spline pyramid (OP) and the stepwise optimal spline pyramid (SOP). Based on the SOP and some techniques similar to those developed by Daubechies, Mallat, and Vetterli [13], [27], [42], we derive a stepwise discrete wavelet transform of l_2 (the stepwise optimal wavelet pyramid SWP). Finally, we use an example to compare the OP and the SWP representations with the Gaussian/Laplacian pyramids that are widely used in computer vision [6].

2. Notation and preliminaries.

2.1. Definitions and notation. The signals considered here are discrete functions with "finite energy." The collection of all such signals constitutes the space of square summable sequences l_2.

The symbol "$*$" will be used for three slightly different binary operations that are defined below: the convolution, the mixed convolution, and the discrete convolution. The ambiguity should be easily resolved from the context.

For two functions f and g defined on $\mathcal{R}$, $*$ denotes the usual convolution:

$$(2) \qquad (f * g)(x) = \int_{-\infty}^{+\infty} f(\xi)g(x - \xi)d\xi, \quad x \in \mathcal{R}.$$

The mixed convolution between a sequence $\{b(k)\}_{k \in \mathcal{Z}}$ and a function f defined on $\mathcal{R}$ is the function $b * f$ defined on $\mathcal{R}$, given by

$$(3) \qquad (b * f)(x) = \sum_{k=-\infty}^{k=+\infty} b(k)f(x - k), \quad x \in \mathcal{R}.$$

The discrete convolution between two sequences a and b is the sequence $a * b$:

$$(4) \qquad (a * b)(l) = \sum_{k=-\infty}^{k=+\infty} a(k)b(l - k), \quad l \in \mathcal{Z}.$$

Whenever it exits, the convolution inverse $(b)^{-1}$ of a sequence b is defined by

$$(5) \qquad \left((b)^{-1} * b\right)(k) = \delta_0(k),$$

where δ_i is the unit impulse located at i ; i.e., $\delta_i(i) = 1$ and $\delta_i(k) = 0$ for $k \neq i$.

We will use the term *Fourier transform* to describe both the usual Fourier transform for functions defined on $\mathcal{R}$:

$$(6) \qquad \hat{g}(f) = \int_{\mathcal{R}} g(x)e^{-i2\pi fx}dx,$$

and the usual Fourier transform for sequences,

$$(7) \qquad \hat{b}(f) = \sum_{i \in \mathcal{Z}} b(k)e^{-i2\pi fk}.$$

A continuous filter $\hat{\lambda}(f)$ is the Fourier transform of a function λ on $\mathcal{R}$ (the impulse response) that defines a bounded convolution operator on L_2:

$$(8) \qquad \lambda : g \in L_2 \to \lambda * g \in L_2.$$

Since the convolution product $\lambda * g$ becomes a multiplication product $\hat{\lambda}\hat{g}$ in Fourier space, the filter $\hat{\lambda}$ selectively alters the frequency components of $\hat{g}$.

A discrete filter $\hat{h}(f)$ is the Fourier transform of a function h on $\mathcal{Z}$ (the impulse response) that defines a bounded convolution operator on l_2:

$$(9) \qquad h : u \in l_2 \to h * u \in l_2.$$

The reflection of a sequence b is the function $b^\vee$, given by

$$(10) \qquad b^\vee(k) = b(-k) \quad \forall k \in \mathcal{Z}.$$

The modulation $\tilde{b}(k)$ of a sequence b is obtained by changing the signs of the odd components of b:

$$(11) \qquad \tilde{b}(k) = (-1)^k b(k).$$

The operator $\downarrow_m$ of down-sampling by the integer factor m assigns to a sequence b the sequence $\downarrow_m [b]$, given by

$$(12) \qquad (\downarrow_m [b])(k) = b(mk) \quad \forall k \in \mathcal{Z}.$$

The operator $\uparrow_m$ of up-sampling by the integer factor m takes a discrete signal b and expands it by adding $m - 1$ zeros between consecutive samples:

$$(13) \qquad (\uparrow_m [b])(k) = \begin{cases} b(k'), & k = mk', \\ 0, & \text{elsewhere.} \end{cases}$$

2.2. The discrete spline spaces $\mathbf{S}_m^n$. We begin by defining the discrete B-spline $b_m^n(k)$ of order n and integer coarseness $m \geq 1$:

$$(14) \qquad b_m^n(k) = \beta^n(k/m) \quad \forall k \in \mathcal{Z},$$

where $\beta^n(x)$ are the continuous symmetrical B-splines of order n. These are obtained by the n-fold convolution of the B-spline of order zero:

$$(15) \qquad \beta^n(x) = (\beta^0 * \beta^0 * \cdots * \beta^0)(x) \qquad (n \text{ convolution}),$$

where $\beta^0(x)$ is the characteristic function in the interval $[-1/2, 1/2)$ (i.e., $\beta^0(x) = 1$ in $[-1/2, 1/2)$ and $\beta^0(x) = 0$ elsewhere). The bell-shaped functions $\beta^n(x)$ have compact support. They were introduced by Schoenberg, who used them to construct a simple basis for the polynomial splines spaces of order n [34].

Using the sequences b_m^n in (14), we define the subspaces $\mathbf{S}_m^n$ of l_2 to be

$$(16) \quad S_m^n := \left\{ v \in l_2 : v(k) = \sum_{i \in Z} c(i) b_m^n(k - mi) = (b_m^n * \uparrow_m [c])(k), \quad c \in l_2 \right\},$$

where n and m are positive integers and where the operator $\uparrow_m$ is defined by (13). As shown in §3, for n odd (which we will assume throughout) the vector spaces $\mathbf{S}_m^n$ are closed subspaces of l_2, and $\mathbf{S}_1^n = l_2$. The discrete functions in $\mathbf{S}_m^n$ are smooth in the sense that they are samples of polynomial spline functions of class C^{n-1}. In this way, the index n is the description of a smoothness constraint. In §3, it is shown that if $m_2 = km_1$ (m_1, m_2, k are positive integers), then $\mathbf{S}_{m_2}^n \subset \mathbf{S}_{m_1}^n$. Thus, in some sense, the index m is related to the coarseness of the spaces $\mathbf{S}_m^n$.

2.3. Review of some results on the continuous fundamental spline filters. The fundamental spline function of order n, $\eta^n(x)$ (also known as cardinal, or interpolating spline) has the value 1 at $x = 0$, and is zero at all the other knot points (the only knot points we consider here are the integers). Thus, it is used to interpolate between data points producing a continuous spline function of order n [4], [28], [34]. Given a discrete signal $s(k)$, its spline interpolation σ^n is given by

$$(17) \qquad \sigma^n(x) = (s * \eta^n)(x) = \sum_{i \in Z} s(i) \eta^n(x - i).$$

Equation (17) states that the polynomial spline interpolant $\sigma^n(x)$ is obtained by filtering the tempered distribution $\sum_{i \in Z} s(i) \delta(x - i)$ with a filter whose impulse response is $\eta^n(x)$. Using Poisson's formula, the Fourier transform of $\eta^n(x)$ is given by

$$(18) \qquad H^n(f) = \frac{(\text{sinc}(f))^{n+1}}{\sum_{i \in Z} (\text{sinc}(f - i))^{n+1}} = \begin{cases} 0, & f \in Z \setminus 0, \\ 1, & f = 0, \\ (1 + U^n(f))^{-1}, & \text{elsewhere}, \end{cases}$$

where $\text{sinc}(x) = \sin(\pi x)/\pi x$ and where $U^n(f)$ is given by

$$(19) \qquad U^n(f) = \begin{cases} \sum_{i=1}^{i=\infty} (i/f + 1)^{-n-1} + (i/f - 1)^{-n-1}, & n \text{ odd}, \\ \sum_{i=1}^{i=\infty} (-1)^i \left((i/f + 1)^{-n-1} - (i/f - 1)^{-n-1} \right), & n \text{ even}. \end{cases}$$

An important feature is that the Fourier transform $H^n(f)$ of $\eta^n(x)$ converges to the ideal lowpass filter; a well-known property [4], [15], [28], [35] stated in the following theorem.

THEOREM 1. *The Fourier transforms of the fundamental spline interpolators $H^n(f)$ converge to the ideal lowpass filter as n goes to infinity pointwise almost everywhere and in $L_p(-\infty, +\infty)$ for all $p \in [1, \infty)$:*

$$(20) \qquad L_p - \lim_{n \to \infty} H^n(f) = \text{rect}(f) = \begin{cases} 1, & |f| < 1/2, \\ 1/2, & |f| = 1/2, \\ 0, & |f| > 1/2. \end{cases}$$

3. Least squares approximation in the spaces $\mathbf{S}_m^n$. Since one of our goals is to find least squares approximations in the spaces $\mathbf{S}_m^n$, we start by studying the properties of $\mathbf{S}_m^n$.

3.1. Properties of $\mathbf{S}_m^n$. First, we prove that the spaces $\mathbf{S}_m^n$ in (16) are well-defined subspaces of l_2 by showing that $b_m^n * \uparrow_m [c] \in l_2$, for all $c \in l_2$. To see this, we note that since β^n has compact support, the sequence b_m^n defined by (14) has finitely many nonzero values. Thus, b_m^n is absolutely summable. This implies that b_m^n defines a bounded convolution operator from l_2 into itself. From this and the fact that the up-sampling operator is an isometry, we get

$$(21) \qquad \|b_m^n * (\uparrow_m [c])\|_{l_2} \leq \|b_m^n\|_{l_1} \|c\|_{l_2} .$$

From the last inequality, it immediately follows that $\mathbf{S}_m^n$, given by (16), are well-defined subspaces of l_2.

There are embedding relations between the spaces $\mathbf{S}_m^n$. These embeddings follow from the well-known embedding properties of the continuous polynomial splines of order n [25], [27], [30].

PROPOSITION 2. *If n is odd, then*

$$(22) \qquad \mathbf{S}_{lm}^n \subset \mathbf{S}_m^n \quad \forall l \in \mathcal{Z}^+.$$

Proof. For n odd, the B-spline $\beta^n(x/lm)$ (where l is a positive integer) is also a polynomial spline with knot points on $m\mathcal{Z}$. Thus, it can be written, in terms of $\beta^n(x/m)$ and a sequence $u \in l_2$, as

$$(23) \qquad \beta^n(x/lm) = \sum_{i \in \mathcal{Z}} u(i) \beta^n \left(\frac{x}{m} - i \right).$$

Both this equality and the definition of b_m^n given by (14) imply that

$$(24) \qquad b_{lm}^n = b_m^n * (\uparrow_m [u]) .$$

We use (24), together with the operator identity

$$(25) \qquad \uparrow_{ml} = \uparrow_m \uparrow_l$$

and the equality

$$(26) \qquad \uparrow_m [v_1] * \uparrow_m [v_2] = \uparrow_m [v_1 * v_2]$$

to get

$$(27) \quad (\uparrow_{lm} [c]) * b_{lm}^n = (\uparrow_{lm} [c]) * (\uparrow_m [u]) * b_m^n = (\uparrow_m [(\uparrow_l [c]) * u] * b_m^n \quad \forall c \in l_2.$$

The Fourier transform of u,

$$(28) \qquad U(f) = l\,\mathrm{sinc}^{n+1}(lf)/\mathrm{sinc}^{n+1}(f),$$

is continuous and bounded above by a constant. Thus, we have

$$(29) \qquad \|\uparrow_l [c] * u\|_{l_2} \leq \mathrm{Const} \, \|c\|_{l_2} .$$

The proof of the proposition then follows from (27) and (29) and from the definition of $\mathbf{S}_m^n$ given by (16).

Since our aim is to find least squares approximations in $\mathbf{S}_m^n$, we need to show that $\mathbf{S}_m^n$ are closed subspaces of l_2—a result that we state in the following theorem.

THEOREM 3. *If n is odd, then $\mathbf{S}_1^n = l_2$ and $\mathbf{S}_m^n$ are closed subspaces of l_2.*

The proof of the theorem relies on the following simple lemma.

LEMMA 4. *Let $B_m^n(f)$ denote the Fourier transform of $b_m^n(k)$. If n is odd, then there exist two positive constants α_1 and α_2 such that*

$$(30) \qquad \alpha_1 \leq B_m^n(f) \quad \forall f \in [-1/2m, 1/2m],$$

$$(31) \qquad B_m^n(f) \leq \alpha_2 \quad \forall f \in \mathcal{R}.$$

Proof. We first note that the Fourier transform of $\beta^0(x)$ is the function $\mathrm{sinc}(f)$. From this fact, Poisson's formula, and the definition of b_m^n (equation (14)), $B_m^n(f)$ can be expressed as

$$(32) \qquad B_m^n(f) = m \sum_{i \in \mathcal{Z}} (-1)^{(n+1)mi} \left(\frac{\sin(m\pi f)}{m\pi(f-i)} \right)^{n+1}$$

Clearly, the function $B_m^n(f)$ is both symmetrical ($B_m^n(f) = B_m^n(-f)$) and periodic with period 1. Since the terms of the series in (32) are continuous and of the order of $|i|^{-n-1}$, it follows that the series in (32) converges uniformly for all $n > 0$ in the interval $f \in [0,1]$. Thus, $B_m^n(f)$ is continuous. Since $B_m^n(f)$ is continuous and periodic, it is bounded above by some constant α_2.

For n odd and for $f \in [0, 1/2m]$, all the terms of the series (32) are nonnegative, and the term for $i = 0$ is strictly positive. Hence, $B_m^n(f)$ is bounded below by a strictly positive constant α_1.

Proof of Theorem 3. To prove that $\mathbf{S}_m^n$ are closed, we show that the operator $b_m^n * \uparrow_m : c \in l_2 \to b_m^n * \uparrow_m [c] \in l_2$ is coercive (i.e., $\|b_m^n * \uparrow_m [c]\|_{l_2} \geq \alpha \|c\|_{l_2}$ for all $c \in l_2$ for some $\alpha > 0$). Taking the Fourier transform of $b_m^n * \uparrow_m [c]$ and using Plancherel's theorem, we get

$$(33) \qquad \|b_m^n * \uparrow_m [c]\|_{l_2}^2 = \int_0^1 |B_m^n(f)\hat{c}(mf)|^2 \, df = m^{-1} \int_0^m |B_m^n(f/m)\hat{c}(f)|^2 \, df,$$

where $B_m^n(f)$ is the Fourier transform of b_m^n. By integrating over intervals of length 1 and using the fact that $\hat{c}(f)$ and $B_m^n(f)$ are periodic with period 1, we rewrite the term following the last equality in (33) to obtain

(34)

$$m^{-1} \int_0^m |B_m^n(f/m)\hat{c}(f)|^2 \, df = m^{-1} \int_0^1 |\hat{c}(f)|^2 \sum_{j=0}^{m-1} |B_m^n(f/m - j/m)|^2 df$$

$$\geq m^{-1} \operatorname*{essinf}_{f \in I = [0,1]} \left(\sum_{j=0}^{m-1} |B_m^n(f/m - j/m)|^2 \right) \|\hat{c}\|_{l_2}^2$$

$$\geq m^{-1} \operatorname*{essinf}_{f \in I = [0,1/2]} \left(|B_m^n(f/m)|^2 \right) \|\hat{c}\|_{l_2}^2.$$

Therefore, the coercivity of the operator $b_m^n * \uparrow_m$ follows directly from (33), (34), and Lemma 4.

3.2. Approximations in $\mathbf{S}_m^n$. Since by Theorem 3 $\mathbf{S}_m^n$ is a closed subspace of l_2, the least squares approximation s_a of s is given by the orthogonal projection on $\mathbf{S}_m^n$. Hence, the error $s - s_a$ is orthogonal to $\mathbf{S}_m^n$. In particular, because of definition (16), the error is orthogonal to b_m^n and to all of its shifted versions at integer multiples of m:

$$(35) \qquad \langle (s - s_a)(k), b_m^n(k - lm) \rangle_{l_2} = 0 \quad \forall l \in \mathcal{Z}.$$

Using the expression of $s_a \in \mathbf{S}_m^n$ given by

$$(36) \qquad s_a(k) = \sum_{i \in \mathcal{Z}} c_a(i) b_m^n(k - mi) = (\uparrow_m [c_a] * b_m^n)(k),$$

we rewrite (35) to get

$$(37) \qquad \langle s(k), b_m^n(k - lm) \rangle_{l_2} = \sum_{i \in \mathcal{Z}} c_a(i) \langle b_m^n(k - im), b_m^n(k - lm) \rangle_{l_2} \quad \forall l \in \mathcal{Z}.$$

Using the fact that b_m^n is symmetric, we can express (37) as the convolution equation

$$(38) \qquad \downarrow_m [b_m^n * s] = c_a * \downarrow_m [b_m^n * b_m^n].$$

This equation can be solved to obtain the unknown sequence c_a. A filtering interpretation of this process is given in [40]. The facts that this procedure is well defined, that the filters are stable, and that equation (37) can be solved follow from the following theorem.

THEOREM 5. *The Fourier transform $T_m^n(f)$ of $t_m^n(l) := \downarrow_m [b_m^n * b_m^n](l)$ is strictly positive. Moreover, $t_m^n \in l_1$, and it has a convolution inverse $(t_m^n)^{-1} \in l_1$ with Fourier transform $(T_m^n(f))^{-1}$ that is also strictly positive.*

Proof. The sequence $t_m^n(l) := \downarrow_m [b_m^n * b_m^n](l)$ has finitely many nonzero values. Thus, $t_m^n \in l_1$, and it defines a bounded convolution operator from l_2 into itself (e.g., $\|t_m^n * c\|_{l_2} \leq \text{Const}\|c\|_{l_2}$). Using the relation between the Fourier transform of a discrete signal $b(k)$ (cf. (7)) and its down-sampled version $\downarrow_m [b]$

$$(39) \qquad (\downarrow_m [b])\widehat{\,}(f) = m^{-1} \sum_{j=0}^{m-1} \hat{b}(f/m - j/m),$$

we obtain the Fourier transform $T_m^n(f)$ of t_m^n:

$$(40) \qquad T_m^n(f) = m^{-1} \sum_{j=0}^{m-1} |B_m^n(f/m - j/m)|^2.$$

The function $T_m^n(f)$ is precisely the sum that appears in the right-hand side of the first inequality in (34). Therefore, Lemma 4 implies that $T_m^n(f)$ is strictly positive and is bounded above by a constant. It follows that $(t_m^n)^{-1} \in l_2$ exists. In fact, since t_m^n has only finitely many nonzero values, $T_m^n(f)$ is a strictly positive trigonometric polynomial. Therefore, $(t_m^n)^{-1}$ decays exponentially fast as $|l| \to \infty$. Hence, $(t_m^n)^{-1}(l)$ is also absolutely summable.

From Theorem 5, t_m^n and $(t_m^n)^{-1}$ define bounded convolution operators on l_2 that are the inverses of each other (cf. (9)). Thus, they are the impulse responses

of the filters $T_m^n(f)$ and $(T_m^n(f))^{-1}$. We use $(t_m^n)^{-1}$ to solve (38) and obtain the approximation s_a:

$$
\begin{aligned}
s_a &= b_m^n * \uparrow_m [c_a] \\
&= b_m^n * \uparrow_m \left[(t_m^n)^{-1} * \downarrow_m [b_m^n * s] \right] \\
&= b_m^n * \uparrow_m \left[\downarrow_m \left[\uparrow_m [(t_m^n)^{-1}] * b_m^n * s \right] \right],
\end{aligned}
$$

(41)

where in the last equality of (41), we have used the functional equality

$$
a * \downarrow_m [b] = \downarrow_m [\uparrow_m [a] * b] \quad \forall a, b \in l_2.
$$

(42)

3.3. Fundamental discrete spline filters. The space $\mathbf{S}_m^n$ (n, m fixed) can be generated by bases other than $\{b_m^n(k - mi)\}_{i \in \mathcal{Z}}$. A complete characterization of all unconditional bases of a given separable Hilbert space as well as a simple way to obtain any particular basis from any other can be found in [1]. In particular, all Riesz bases for $\mathbf{S}_m^n$ can be characterized in term of $\{b_m^n(k - mi)\}_{i \in \mathcal{Z}}$ by appropriate "linear combinations." For instance, it is not difficult to show that if we sample the Battle/Lemarié spline scaling function $\phi^n(x/m)$ on $\mathcal{Z}$, we obtain the sequence $l_m^n = \uparrow_m [(b_1^{2n+1})^{-1/2}] * b_m^n$. The set $\{l_m^n(k - mi)\}_{i \in \mathcal{Z}}$ is also a basis for $\mathbf{S}_m^n$. However, it does not form an orthogonal basis of $\mathbf{S}_m^n$. The orthogonal basis is given by $\{o_m^n(k - mi)\}_{i \in \mathcal{Z}}$ generated by $o_m^n = \uparrow_m [(t_m^n)^{-1/2}] * b_m^n$.

A particular basis of interest is the fundamental basis $\{h_m^n(k - mi)\}_{i \in \mathcal{Z}}$, in which the representation of any sequence $s(k) \in \mathbf{S}_m^n$ is directly obtained from the sequence values $\{s(mi)\}_{i \in \mathcal{Z}}$:

$$
s(k) = \sum_{i \in \mathcal{Z}} s(mi) h_m^n(k - mi) = \uparrow_m \downarrow_m [s] * h_m^n.
$$

(43)

The fundamental sequence $h_m^n(k)$ is obtained by sampling the continuous fundamental spline filter $\eta^n(x)$, defined at the beginning of §2.3:

$$
h_m^n(k) = \eta^n(k/m) \quad \forall k \in \mathcal{Z}.
$$

(44)

The sequence $h_m^n(k)$ is the linear combination of $b_m^n(k)$ given by [38]:

$$
h_m^n = \uparrow_m [(b_1^n)^{-1}] * b_m^n.
$$

(45)

The existence of $(b_1^n)^{-1}$ follows from Lemma 4. In fact, since b_1^n has finitely many nonzero values, it follows that $(b_1^n)^{-1}$ decays exponentially fast. Thus, both b_1^n and $(b_1^n)^{-1}$ are in $\in l_1$. The fact that $\{h_m^n(k - mi)\}_{i \in \mathcal{Z}}$ is a basis of $\mathbf{S}_m^n$ follows immediately from the definition of $\mathbf{S}_m^n$, Lemma 4, and equations (26) and (45).

Using identity (26), we manipulate (41) so as to exhibit h_m^n. We get

$$
s_a = h_m^n * \uparrow_m \left[\downarrow_m \left[\overset{\circ}{h}_m^n * s \right] \right],
$$

(46)

where

$$
\overset{\circ}{h}_m^n = \uparrow_m [(t_m^n)^{-1} * b_1^n] * b_m^n.
$$

(47)

From (46), it is not difficult to see that h_m^n and $\overset{\circ}{h}_m^n$ are biorthogonal [11]:

$$
\downarrow_m \left[\overset{\circ}{h}_m^n * h_m^n \right] (k) = \delta_0(k) \quad \forall k \in \mathcal{Z}.
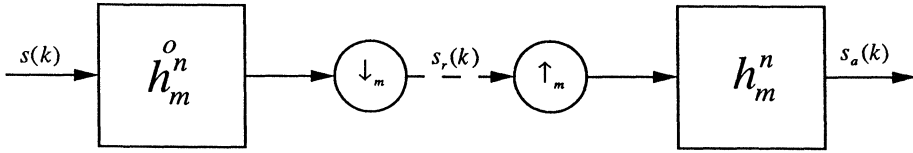$$

(48)

FIG. 1. *Schematic representation of the least squares approximation in* S_m^n.

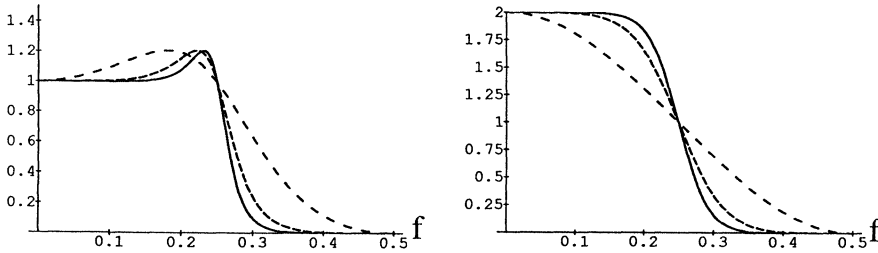(A) Optimal prefilters   (B) Interpolating postfilters

FIG. 2. *Least squares spline filters.* (A) *Prefilters* $\mathring{H}_2^1(f)$ (- - - -), $\mathring{H}_2^3(f)$ (- - - -), *and* $\mathring{H}_2^5(f)$ (*continuous line*).

Similar to Hummel [22], we can interpret $\mathring{h}_m^n$ to be the optimal prefilter needed before the interpolator h_m^n, given by (45). The process that can be used to determine the best approximation of a signal in S_m^n is illustrated in Fig. 1. In effect, this procedure is equivalent to prefiltering the data with $\mathring{h}_m^n$, down-sampling by a factor m, then up-sampling by m and applying a discrete fundamental spline interpolation. The frequency responses of the filters ($n = 1, 3, 5$ and $m = 2$) used in our procedure are shown in Fig. 2. The graphs show that the lowpass characteristics of these filters improve with n. This behavior will be analyzed in more detail in the next section.

4. Asymptotic properties of the filters. We will show that for m fixed, the prefilters $\mathring{H}_m^n(f)$ and the interpolating filters $H_m^n(f)$ tend pointwise and in $L_2(-1/2, 1/2)$ to an ideal discrete lowpass filter with periodic support in $\bigcup_{j \in \mathcal{Z}}[j - 1/2m, j + 1/2m]$.

These convergence properties are described in the following theorem.

THEOREM 6. *For* n *odd, the prefilter* $\mathring{H}_m^n(f)$ *converges in* $L_2(-1/2, 1/2)$ *and pointwise almost everywhere to an ideal discrete lowpass filter* Prect_m (*the periodic rectangular pulse*) *as* n *tends to infinity:*

$$(49) \qquad \lim_{n \to \infty} \mathring{H}_m^n(f) = \begin{cases} 1, & |f| < 1/2m, \\ 1/2, & |f| = 1/2m, \\ 0, & 1/2m < |f| < 1. \end{cases}$$

Similarly, for n *odd, the interpolating filter* $H_m^n(f)$ *converges in* $L_2(-1/2, 1/2)$ *and pointwise almost everywhere to an ideal discrete lowpass filter with gain* m *as* n *tends to infinity:*

$$(50) \qquad \lim_{n \to \infty} H_m^n(f) = m \, \text{Prect}_m(f).$$

Using Plancherel's Theorem, we immediately obtain the following corollary.

COROLLARY 7. *For n odd, the impulse responses $\overset{\circ}{h}{}^n_m(k)$ converge in l_2 to the ideal discrete interpolator, $D\mathrm{sinc}_m(k) = \mathrm{sinc}(k/m)$ with $k \in \mathcal{Z}$, as n tends to infinity.*

Similarly, for n odd, the interpolators $h^n_m(k)$ converge in l_2 to the ideal discrete interpolators with gain m, $mD\mathrm{sinc}_m(k)$, as n tends to infinity.

These results are conceptually interesting because they provide the link with Shannon's sampling theory [2], [4], [5], [7], [17], [18], [20], [24], [31], [39], [46]. In particular, for the case of uniform sampling, Shannon's sampling paradigm for non-bandlimited signals states that a signal must first be prefiltered by an ideal filter before sampling and that the signal "reconstruction" is obtained by an ideal post-filtering. The approximation in $\mathbf{S}^n_m$ gives rise to the same structure as illustrated by Fig. 1. It consists of a prefiltering with $\overset{\circ}{H}{}^n_m$, followed by down-sampling by a factor m. This first step gives an m fold reduction in the data. The approximation is then obtained by up-sampling and postfiltering with H^n_m. Moreover, in the limit, all the filters converge to discrete ideal filters. Similar results for the analog polynomial spline case can be found in [4], [39]. The general case for analog functions is described in [2].

The above asymptotic results also explain the appearance of Gibbs oscillations which occur when sequences are approximated by elements in spaces $\mathbf{S}^n_m$ with sufficiently high smoothing order n.

Proof of Theorem 6. Symmetry allows us to restrict our attention to the frequency interval $f \in [0, 1/2)$. The Fourier transform of b^n_m is given by

$$(51) \qquad B^n_m(f) = m \sum_{i \in \mathcal{Z}} \mathrm{sinc}^{n+1}(m(f-i)).$$

We use (39) and (40) in conjunction with the fact that the Fourier transform of a discrete signal is periodic with period 1. We also use $(\uparrow_m [b])\widehat{\ }(f) = \hat{b}(mf)$ to express the Fourier transform of $\uparrow_m [(t^n_m)^{-1}]$ and $\uparrow_m [b^n_1] = \uparrow_m [\downarrow_m [b^n_m]]$ in terms of $B^n_m(f)$ as

$$(52) \qquad (\uparrow_m [b^n_1])\widehat{\ }(f) = m^{-1} \sum_{j=L}^{L+m-1} B^n_m(f - j/m),$$

$$(53) \qquad (\uparrow_m [(t^n_m)^{-1}])\widehat{\ }(f) = \frac{m}{\sum_{j=L}^{L+m-1} |B^n_m(f - j/m)|^2},$$

where L is an arbitrary integer. Using (51)–(53), we obtain the Fourier transform $\overset{\circ}{H}{}^n_m(f)$ of $\overset{\circ}{h}{}^n_m$:

$$(54) \qquad \overset{\circ}{H}{}^n_m(f) = \frac{B^n_m(f) \sum_{j=L}^{L+m-1} B^n_m(f - j/m)}{\sum_{j=L}^{L+m-1} |B^n_m(f - j/m)|^2}.$$

Using (51), (18) and straightforward trigonometric identities, (54) can be written as

$$(55) \quad \overset{\circ}{H}{}^n_m(f) = (H^n(f))^{-1} \frac{\sum_{j=L}^{L+m-1} (-1)^j (1 - j/mf)^{-n-1} (H^n(f - j/m))^{-1}}{\sum_{j=L}^{L+m-1} (1 - j/mf)^{-2n-2} (H^n(f - j/m))^{-2}},$$

where $H^n(f)$ is the Fourier transform of the continuous fundamental spline function of order n given by (18). We choose L in (55) to be $L = -(m-1)/2$ if m is odd, and $L = -(m/2 - 1)$ if m is even. With this choice, we take limits in (55) to get

$$(56) \quad \lim_{n \to \infty} \overset{\circ}{H}{}^n_m(f) = \lim_{n \to \infty} \frac{\sum\limits_{j=L}^{L+m-1} (-1)^j (1 - j/mf)^{-n-1}}{\sum\limits_{j=L}^{L+m-1} (1 - j/mf)^{-2n-2}} = 1 \quad \forall f \in (0, 1/2m).$$

We use Schwarz's inequality on (55) to get the estimate

$$(57) \quad \left| \overset{\circ}{H}{}^n_m(f) \right| \le m^{1/2} |H^n(f)|^{-1} \left(\sum_{j=L}^{L+m-1} (1 - j/mf)^{-2n-2} \left(H^n(f - j/m)\right)^{-2} \right)^{-1/2}.$$

For $f \in (1/2m, 1/2)$, it follows from (57) and Theorem 1 that $\overset{\circ}{H}{}^n_m(f)$ converges pointwise to 0 as n tends to infinity. Moreover, (57) yields the upper bound

$$(58) \qquad \left| \overset{\circ}{H}{}^n_m(f) \right| \le m^{1/2}.$$

Because of Lebesgue's dominated convergence theorem, equations (56)–(58) imply that $\overset{\circ}{H}{}^n_m(f)$ tends to $Prect_m(f)$ in $L_2(-1/2, 1/2)$.

To prove the second part of the theorem, we first note that $H^n_m(f)$ is given by

$$(59) \qquad H^n_m(f) = \frac{B^n_m(f)}{(\uparrow_m [b^n_1]) \widehat{}(f)}.$$

From (51) and for n odd, it can be seen that

$$(60) \qquad B^n_m(f) = m^{-n} B^n_1(f) \left(\frac{\sin(m\pi f)}{\sin(\pi f)} \right)^{n+1}.$$

Using the fact that $(\uparrow_m [b]) \widehat{}(f) = \hat{b}(mf)$, and using expressions (18) and (60), we simplify (59) to obtain

$$(61) \qquad H^n_m(f) = \frac{B^n_m(f)}{B^n_1(mf)} = m^{-n} \left(\frac{\sin(m\pi f)}{\sin(\pi f)} \right)^{n+1} \frac{B^n_1(f)}{B^n_1(mf)} = m \frac{H^n(mf)}{H^n(f)}.$$

The last equality in (61) and Theorem 1 together yield the pointwise convergence. For n odd, a simple estimate derived for $H^n(f)$ (cf. (18) and (19)) yields that for $f \in (-1/2, 1/2)$, $1/2 < H^n(f) < 1$. Hence, from (61) we get

$$(62) \qquad |H^n_m(f)| \le 2m,$$

which implies the $L_2(-1/2, 1/2)$ convergence of $H^n_m(f)$ to the ideal discrete filter $Prect_m(f)$ with gain m and periodic support in $\bigcup_{j \in \mathcal{Z}} [j - 1/2m, j + 1/2m]$.

5. Multiresolution pyramids and step-by-step discrete wavelet transform.

5.1. The optimal and stepwise optimal discrete spline pyramids.

A multiresolution pyramid representation of a discrete signal consists of several versions of the signal at different resolution levels. The name pyramid derives from the fact that the low-resolution levels are described by fewer samples than their high-resolution counterparts. In applied mathematics and image processing, multiscale representations have been used to find efficient algorithms that start computations at coarse levels and subsequently refine them at finer levels [19], [36].

A multiresolution representation of a signal is commonly obtained by the repeated application of a filtering and a down-sampling to produce the pyramid layers. The Gaussian pyramid for images [6] is an example in which each pyramid level is obtained from the previous one by applying a Gaussian filter and down-sampling each row and column of the image by a factor of 2. A shortcoming of this method is that it does not attempt to minimize the loss of information that occurs when one signal is approximated by another at a coarser resolution. Using (46), we can circumvent this limitation, and produce a multiscale representation that optimizes the fine-to-coarse conversion error. For m fixed, we interpret (46) as representing a signal at a lower resolution: the signal s is prefiltered by $\overset{\circ}{h}{}^n_m$, and only one sample out of m is then retained. This sequence is then up-sampled (cf. (13)) and filtered with h^n_m to obtain the best approximation s_a in $\mathbf{S}^n_m$. In effect, the signal $s_r = \downarrow_m [\overset{\circ}{h}{}^n_m * s]$ contains in a compressed form (factor of compression equal to m) all the information needed to reconstruct the approximation s_a. Hence, by selecting a sequence of integers $\{m = p^j\}_{j=1,\ldots,N.}$, we can use equation (46) to obtain a multiresolution pyramid $\{s_{r(j)}\}_{j=1,\ldots,N.}$:

$$(63) \qquad \begin{cases} s_{r(j)} = \downarrow_{p^j} \left[\overset{\circ}{h}{}^n_{p^j} * s \right], & j = 1,\ldots,N; \\ s_{r(0)} = s. \end{cases}$$

We have used the notation $s_{r(j)}$ to represent level j $(m = p^j)$ of the pyramid in (63), which is obtained by filtering the signal s with $\overset{\circ}{h}{}^n_{p^j}$ and then decimating with a factor equal to p^j. More importantly, since $\mathbf{S}^n_{p^{j+1}} \subset \mathbf{S}^n_{p^j}$ (cf. Proposition 2), the filter used to produce the signal $s_{r(j+1)}$ from $s_{r(j)}$ at the previous resolution level can be obtained by using (46) and the fact that for any sequence b, we have that

$$(64) \qquad \downarrow_{p^{j+1}} [b] = \downarrow_p \left[\downarrow_{p^j} [b] \right].$$

The signal $s_{r(j+1)}$ is given by the following.

  The optimal pyramid (OP):

$$(65) \qquad \begin{aligned} s_{r(j+1)} &= \downarrow_p \left[\overset{\circ}{h}{}^n_p * x_{r(j)} \right], \\ x_{r(j)} &= k^n_{p^j} * s_{r(j)}, \end{aligned}$$

where the operators $k^n_{p^j}$ is given by

$$(66) \qquad k^n_{p^j} = \uparrow_p \left[\left(t^n_{p^{j+1}} \right)^{-1} * t^n_p \right] * \downarrow_{p^j} \left[h^n_{p^j} * h^n_{p^j} \right].$$

Remark 1. Given a regular function $\sigma(x) \in L_2$ with sufficient decay, it can be approximated by an analog spline $\sigma_{p^j}^n(x)$ with knot points on $p^j \mathcal{Z}$. The analog spline approximation $\sigma_{p^j}^n(x)$ that minimizes the l_2-error $\sigma(k) - \sigma_{p^j}^n(k)$ computed at the integer points $\mathcal{Z}$ can be obtained from (63) or from algorithm OP: $\sigma_{p^j}^n(x) = \sum_{k \in \mathcal{Z}} \sigma_{r(j)}(k) \eta^n(x/p^j - k)$, where $\eta^n(x)$ is the interpolating spline as in §2.3. Thus, the approximation problem in $\mathbf{S}_{p^j}^n$ consists of finding a coarse polynomial spline approximation that minimizes the discrete l_2-norm of the error at the integers instead of the usual minimization of the L_2-norm on $\mathcal{R}$.

The error $e_{(j)} = s - s_a = s - h_{p^j}^n * \uparrow_{p^j} \left[s_{r(j)} \right]$ between the original signal and its approximation is the smallest error in l_2 that can be obtained for approximations of s in $\mathbf{S}_{p^j}^n$. However, a drawback of this representation is that the filter $k_{p^j}^n$ in (65) depends upon the resolution level j. On the other hand, the first equation of (65) is independent of the resolution level, and is precisely the first pyramid level for the representation of the signal $x_{r(j)}$. This observation suggests an alternative algorithm for a multiresolution representation of a signal based on the first equation of (65) only.

The stepwise optimal pyramid (SOP):

$$(67) \qquad \begin{aligned} \breve{s}_{r(j+1)} &= \downarrow_p \left[\overset{\circ}{h}_p^n * \breve{s}_{r(j)} \right] \\ \breve{s}_{r(0)} &= s. \end{aligned}$$

If (67) is used instead of (65) for the pyramidal representation of s, then the error $\breve{e}_{(j)} = s - h_{p^j}^n * \uparrow_{p^j} \left[\breve{s}_{r(j)} \right]$ is always larger than or equal to the error $e_{(j)} = s - s_a$. The question of how the two algorithms (65) and (67) compare is partially answered by the following theorem.

THEOREM 8. *For n odd, the filter $K_{p^j}^n(f)$ corresponding to $k_{p^j}^n$ converges in $L_2(-1/2, +1/2)$ and pointwise almost everywhere to a discrete allpass filter as n tends to infinity:*

$$(68) \qquad \lim_{n \to \infty} K_{p^j}^n(f) = 1 \quad \forall f \in \mathcal{R}.$$

The proof of this theorem will be omitted, since, except for the use of the identity

$$(69) \qquad [b_p^n] = \downarrow_{p^j} [b_{p^{j+1}}^n],$$

it is not very different from the proof of Theorem 6.

Heuristically, the above result states that for sufficiently large n the optimal multiresolution algorithms (65) can be replaced by the simpler and more practical algorithm (67), with only minor differences in the outcome. The advantage of the stepwise optimal algorithm is that the passage from one level to the next always uses the same algorithm, and can therefore be implemented using a fast recursive filtering similar to the one described in [41].

5.2. A stepwise discrete wavelet representation. The pyramids discussed in the previous sections are redundant. For instance, the stepwise optimal pyramid OP is redundant because it consists of the signal itself ($s = s_{r(0)}$), to which N copies are added that are of increasingly coarser resolution: $P = \left\{ s_{r(0)}, s_{r(1)}, \ldots, s_{r(N)} \right\}$. The redundant information coincides with the data $s_{r(1)}, \ldots, s_{r(N)}$ and, for $m = 2$, the number of additional samples is approximately equal to the size of $s = s_{r(0)}$. In the case $m = 2$, which is a case of practical interest, we will derive a nonredundant representation equivalent to the SOP pyramid. The main idea is to find a suitable

representation of $(\mathbf{S}_2^n)^\perp$, the orthogonal complement of $\mathbf{S}_2^n$, analogous to (16). To do this, we use techniques similar to the ones developed by Daubechies, Mallat, and Vetterli [13], [27], [42]. We start by defining the discrete function w_2^n and the corresponding space $\mathbf{O}_2^n$ associated with it:

$$(70) \qquad w_2^n(k) = (-1)^{k+1} b_2^n(k+1).$$

$$(71) \quad \mathbf{O}_2^n := \left\{ v \in l_2 : v(k) = \sum_{i \in \mathcal{Z}} c(i) w_2^n(k-2i) = (w_2^n * \uparrow_2 [c])(k), \quad c \in l_2 \right\}.$$

We have the following result.

THEOREM 9. *The space* $\mathbf{O}_2^n$ *is the orthogonal complement of* $\mathbf{S}_2^n$ *in* l_2: $\mathbf{O}_2^n = (\mathbf{S}_2^n)^\perp$.

Before proving this theorem, we first note that the function w_2^n is the discrete equivalent of a continuous wavelet, as defined in [13], [27]; however, in this case w_2^n is not orthogonal to a shifted version of itself. An important point is that the error signal $d_{a(1)} = s - s_a$, resulting from approximating s by $s_a \in \mathbf{S}_2^n$, can be obtained by filtering, as in §3.2:

$$(72) \qquad d_a = w_2^n * \uparrow_2 \left[(t_2^n)^{-1} * \downarrow_2 \left[(w_2^n)^\vee * s \right] \right] = \delta_1 * \tilde{h}_2^n * \uparrow_2 \left[\downarrow_2 \left[\delta_{-1} * \overset{\circ}{\tilde{h}}_2^n * s \right] \right],$$

where the reflection operator " $\vee$ " and the modulation operator " $\sim$ " are defined by (10) and (11), respectively, in §2.

Proof. First, we show that $w_2^n(k-2i)$ is orthogonal to $b_2^n(k)$ by showing that $\downarrow_2 \left[(w_2^n)^\vee * b_2^n \right] = 0$ (where $(w_2^n)^\vee(k) = w_2^n(-k)$). Using (39) and the properties of the Fourier transform, we obtain

$$(73)$$

$$\begin{aligned}
(\downarrow_2 [(w_2^n)^\vee * b_2^n])\widehat{\,}(f) &= \frac{1}{2} \left(B_2^n(f/2)\overline{W_2^n(f/2)} + B_2^n(f/2 - 1/2)\overline{W_2^n(f/2 - 1/2)} \right) \\
&= \frac{1}{2} e^{-i\pi f} (B_2^n(f/2)B_2^n(f/2 - 1/2) \\
&\qquad\qquad - B_2^n(f/2 - 1/2)B_2^n(f/2 - 1)) \\
&= \frac{1}{2} e^{-i\pi f} (B_2^n(f/2)B_2^n(f/2 - 1/2) - B_2^n(f/2 - 1/2)B_2^n(f/2)) \\
&= 0,
\end{aligned}$$

where $\overline{W_2^n(f)}$ denotes the complex conjugate $W_2^n(f)$, which is the Fourier transform of $w_2^n(k)$. It only remains to show that any element $s \in l_2$ can be written as a sum of its least squares approximations in $\mathbf{S}_2^n$ and in $\mathbf{O}_2^n$. We sum the Fourier transforms of d_a and s_a, which are the approximations of s in $\mathbf{O}_2^n$ and $\mathbf{S}_2^n$, respectively; we then use (39), the second equation in (72), periodicity, and Lemma 4 to obtain

$$(74)$$

$$\begin{aligned}
\hat{d}_a(f) + \hat{s}_a(f) &= B_2^n(f - 1/2)\frac{B_2^n(f - 1/2)S(f) - B_2^n(f - 1)S(f - 1/2)}{|B_2^n(f - 1/2)|^2 + |B_2^n(f - 1)|^2} \\
&\quad + B_2^n(f)\frac{B_2^n(f)S(f) + B_2^n(f - 1/2)S(f - 1/2)}{|B_2^n(f - 1/2)|^2 + |B_2^n(f)|^2} \\
&= \hat{s}(f),
\end{aligned}$$

from which the proof follows.

Using (72), we derive the difference or detail representation $\left\{d_{r(j)}\right\}_{j=1,\ldots,N}$:

The stepwise wavelet pyramid (SWP).

$$(75) \quad \begin{cases} \breve{d}_{r(j+1)} = \downarrow_2 \left[\delta_{-1} * \tilde{\overset{\circ}{h}}_2^n * \breve{s}_{r(j)}\right] \\ \breve{s}_{r(j+1)} = \downarrow_2 \left[\overset{\circ}{h}_2^n * \breve{s}_{r(j)}\right] \\ \breve{s}_{r(0)} = s. \end{cases}$$

From Theorem 9 and (46), (72), and (75), it can be seen that the SOP representation is obtained from the SWP pyramid by the iterative algorithm:

The stepwise wavelet decomposition.

$$(76) \quad \breve{s}_{r(N-j)} = h_2^n * \uparrow_2 \left[\breve{s}_{r(N-j+1)}\right] + \delta_1 * \tilde{h}_2^n * \uparrow_2 \left[\breve{d}_{r(N-j+1)}\right], \qquad j = 1, \ldots, N.$$

Remark 2.

(i) The algorithms (75) and (76) constitute a biorthogonal, perfect reconstruction filter bank [33], [43].

(ii) There are two corresponding analog scaling functions $\varphi_{h_2^n}$ and $\varphi_{\overset{\circ}{h}_2^n}$, and two analog biorthogonal wavelets $\psi_{\tilde{h}_2^n}$ and $\psi_{\overset{\circ}{h}_2^n}$, for which the associated L_2 analysis of analog functions defined on $\mathcal{R}$ via nonorthogonal projections is exactly obtained by (75) and (76) (cf. [11]). Obviously, $\varphi_{\overset{\circ}{h}_2^n}$ and $\psi_{\overset{\circ}{h}_2^n}$ are not polynomial splines.

(iii) There are infinitely many basis functions for $\mathbf{S}_m^n$ (cf. §3.3). For each basis, it is possible to obtain a step-by-step wavelet decomposition (or a perfect reconstruction, biorthogonal filter banks) similar to (75) and (76). However, they will not be a good approximation to OP in general.

(iv) Two basis functions generating the same space $\mathbf{S}_m^n$ do not correspond to analog scaling functions that generate the same space; e.g., the scaling functions $\varphi_{h_2^n}$ and $\varphi_{b_2^n}$ associated with h_2^n and b_2^n do not generate the same multiresolution space V_0, even though b_2^n and h_2^n generate the same space $\mathbf{S}_2^n$.

(v) If we choose the biorthogonal filter bank decomposition using the orthogonal basis o_2^n in §3.3 instead of h_2^n, then the corresponding stepwise wavelet algorithms are precisely the Mallat wavelet decomposition and reconstruction algorithms for the analog scaling function $\phi(x)$ associated with the QMF o_2^n [27]. In this case, there exists an underlying discrete multiresolution $E_{2j}^n \neq \mathbf{S}_{2j}^n$, for which these algorithms give the best l_2 approximation of a sequence $s(k)$ in E_{2j}^n [33]. These are also the analysis/synthesis algorithms for the L_2 multiresolution wavelet $V_j(\phi)/W(\phi)$, corresponding to the function ϕ associated with o_2^n. However, ϕ is not a spline function. Moreover, this algorithm does not correspond to the same analog multiresolution $V(\varphi_{h_2^n})$ (see the previous remark, (iv)). For the interpretation of (75) and (76) we refer to §3, Remark 1 in §5.1, and Theorem 8.

6. Experiments. Although the filters used in (65), (67), and (75) have an infinite impulse response, they can still be implemented exactly using the recursive algorithm described in [41]. An alternative approach is to use a standard finite impulse response (FIR) implementation with truncated filters. In the latter case, the computation is approximate, but the error is easily controlled by choosing an appropriate number of coefficients. Table 1 gives those filter coefficients for the cases $n = 1$

TABLE 1
Filters' coefficients for $n = 1$ and $n = 3$.

	$\overset{\circ}{h}{}_2^1$	h_2^1	$\overset{\circ}{h}{}_2^3$	h_2^3
$k = 0$	0.707107	1	0.596797	1
$1, -1$	0.292893	0.5	0.313287	0.600481
$2, -2$	−0.12132	0	−0.082769	0
$3, -3$	−0.0502525	0	−0.0921993	−0.127405
$4, -4$	0.0208153	0	0.0540288	0
$5, -5$	0.00862197	0	0.0436996	0.034138
$6, -6$	−0.00357134	0	−0.0302508	0
$7, -7$	−0.0014793	0	−0.0225552	−0.00914725
$8, -8$	0.000612745	0	0.0162251	0
$9, -9$		0	0.0118738	0.002451
$10, -10$		0	−0.00861788	0
$11, -11$		0	−0.00627964	−0.000656743
$12, -12$		0	0.00456713	
$13, -13$		0	0.00332464	
$14, -14$		0	−0.00241916	
$15, -15$		0	−0.00176059	
$16, -16$		0	0.00128128	
$17, -17$		0	0.000932349	
$18, -18$		0	−0.000678643	

and $n = 3$. In our experiments, we used the first of these approaches. To avoid border effects and discontinuities, we have used the common practice of extending the signals/images at the boundaries by taking their mirror images.

We have performed three experiments on a test image, the MRI image. First we compared different approximations of the image by varying the parameters n and m in the approximation spaces $\mathbf{S}_m^n$. To assess the appropriateness of the approximation we used the signal-to-noise ratio [23] associated with the approximation s_a, as defined by

$$(77) \qquad SNR = 20 \log \left(\frac{|\sup(s) - \inf(s)|}{\|s - s_a\|_{l_2}} \right).$$

Table 2 gives the measurements of the SNR for values of $m = 2, \ldots, 8$ and $n = 1, 3$. These measurements show that for fixed value of m, the SNR for $n = 3$ is higher than for $n = 1$. The improvement seems to saturate quickly, and we anticipate no significant gain for values of n larger than 5. This conclusion is consistent with the convergence results given in Theorem 6, which indicate that the approximation process tends to an ideal filtering process for increasing values of n. As a consequence, higher orders of n will, in general, improve the SNR for images with a predominance of lower frequency components.

Our second experiment was a comparison of the two multiresolution representations OP and SOP. Table 3 gives the values of the SNR for a multiresolution representation of the MRI obtained by the optimal algorithm (67) for the case $p = 2$, $j = 1, 2, 3$, and $n = 1, 3$. Obviously, the two algorithms are equivalent for the determination of level 1. As predicted, the SNR measured for the approximations obtained using the optimal algorithm OP are higher than those obtained form the stepwise optimal algorithm SOP. However, as predicted by Theorem 8, the difference between the two SNRs are small, particularly for the largest value of $n = 3$. Indeed, these differences (which are of the order of 0.01 dB) are very small if compared to the degradation of

TABLE 2

Approximation error (in dB) evaluated for m = 1, 2, ..., 8 and n = 1, 3 in terms of the signal-to-noise ratio for the MRI image.

	$n = 1$	$n = 3$
$m = 2$	32.65	35.39
$m = 3$	27.84	29.08
$m = 4$	24.95	25.58
$m = 5$	23.22	23.73
$m = 6$	22.30	22.68
$m = 7$	21.22	21.62
$m = 8$	20.54	20.85

TABLE 3

Comparison between the optimal pyramid and the stepwise optimal pyramid representations in term of the signal-to-noise ratio (in dB) for the MRI image.

	$n = 1$		$n = 3$	
	OP	SOP	OP	SOP
Level-1	32.65	32.65	35.39	35.39
Level-2	24.95	24.93	25.58	25.57
Level-3	20.54	20.50	20.85	20.83

the SNR between two successive levels, which is of the order of 5dB-10 dB. In fact, the SNR differences in our experiment are negligible, and the results are much better than we had expected.

We compared our multiresolution representation given by the SOP algorithm (67) to the Laplacian pyramid LP which was developed for compact image coding [6]. Each level in the difference-image pyramid consists of the difference between the image at one level and its interpolated version at the next lower level. In other words, each layer of such a pyramid represents the loss of information between a level and its approximation at the coarser level. For this experiment we chose the value $n = 3$, $p = 2$, and $j = 1, 2, 3$ in the SOP algorithm. Fig. 3 shows the difference images for the two representations, with the same intensity scaling to facilitate comparison. For the initial LP, there is significant information at each level, and the initial image is still easily recognizable. In the case of the SOP, the energy in the difference is reduced drastically, and only very high-frequency details are visible. This improvement can be applied advantageously to progressive image transmission. For lossless image coding, the number of bits per pixel (bit-rate) necessary to transmit the bottom of the pyramid up to level j is approximately

$$(78) \qquad\qquad B_j = \sum_{i=j}^{N} H_i 4^{i-1},$$

where H_i denotes the entropy at the ith level of the Laplacian pyramid, and N is the depth of the pyramid. The corresponding rate-distortion curves for our test image are given in Fig. 4. The customary measure of distortion that is used for this type of experiment is the relative mean square error in percent of the total signal energy, as measured on the finer scale. Clearly, the SOP achieves the best performance at all resolution levels. Thus, for the comparable compression factor, we can gain image quality when the SOP is used instead of the LP representation.

Finally, Fig. 5 displays an equivalent SWP representation of the same MRI image. This decomposition was obtained by successive processing along the rows and columns
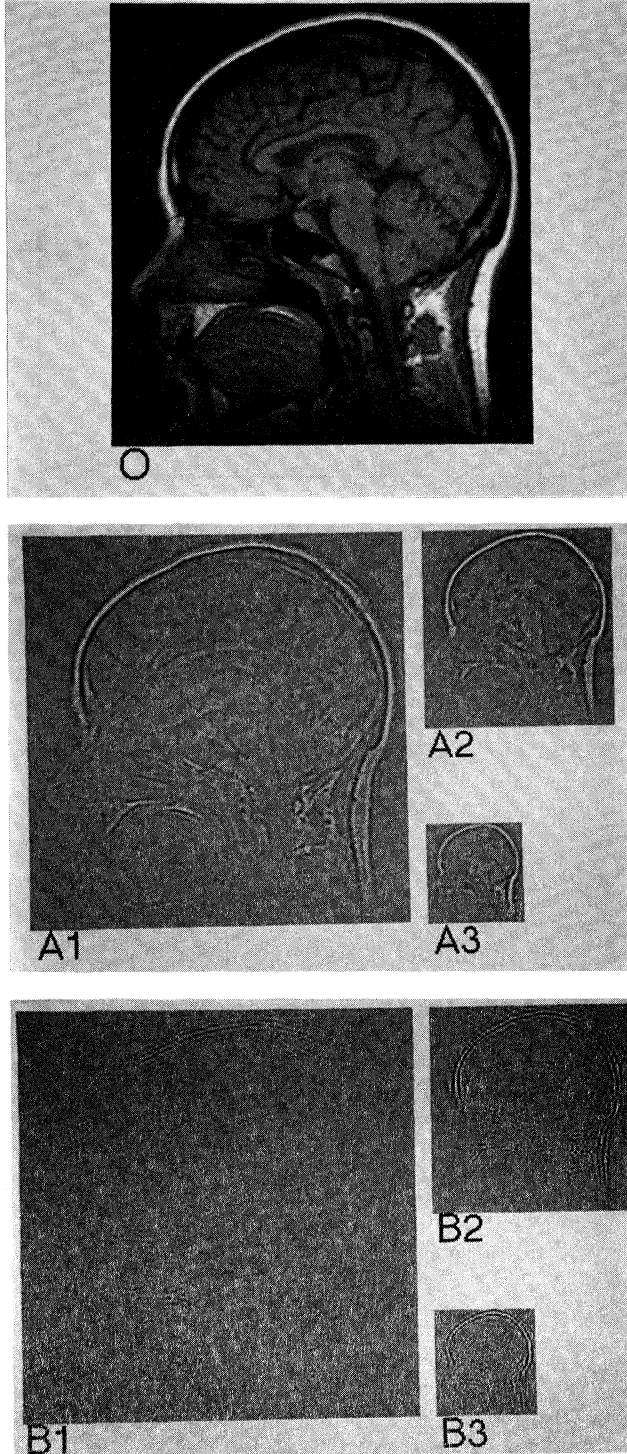
FIG. 3. *Error images between two consecutive levels of the* SOP *pyramid and the Laplacian pyramid* LP *for the* MRI *image* O. (A1-A3) *error/difference images of the Laplacian pyramid.* (B1-B3) *error/difference images of the* SOP *pyramid* ($n = 3$).
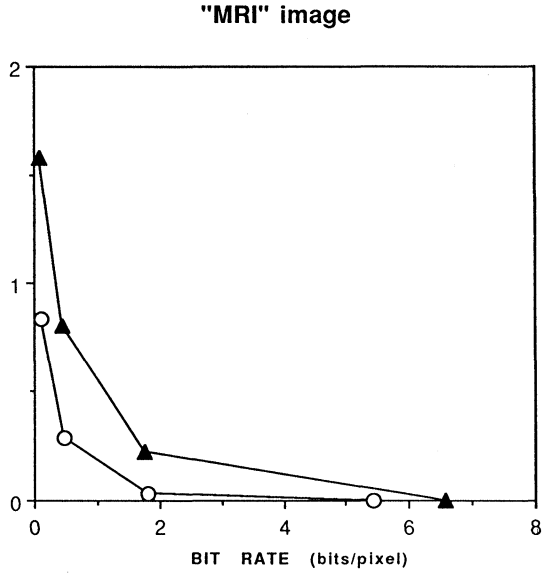
"MRI" image

FIG. 4. *Rate distortion* (MSE) *as a function of the number of bits per pixel needed for lossless transmission up to level* i: SOP (*circle*) *and* LP (*triangle*).
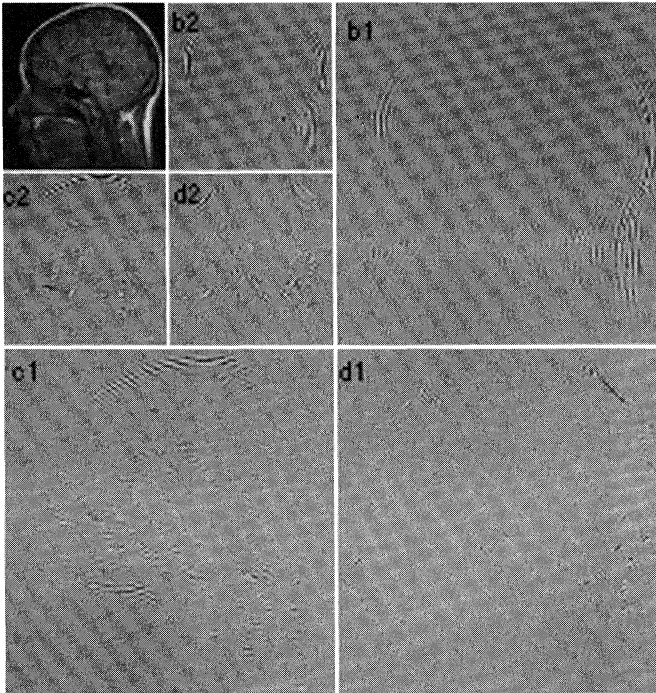

FIG. 5. *The stepwise wavelet representation of the* MRI *image with a level depth 2* (*i.e.,* $m = 2^j$, $j = 1, 2$) *with* $n = 3$.

of the data, following the separable technique first described by Vetterli in [42]. We note that the three quadrants b_1, c_1, and d_1 provide a compressed representation of the difference at level 1 in the SOP (image A1). Likewise, the difference at level 2 (image A2) is represented by the wavelet components b_2, c_2, and d_2. The component in a_2 is precisely the SOP approximation after two iterations (level 2). The decomposition is clearly nonredundant; and, as expected, we have experimentally tested that the original image can be fully recovered from the stepwise pyramid without error. This wavelet decomposition can be used for both image compression and for coding, as described in [12], [16], and [42].

REFERENCES

[1] A. ALDROUBI AND M. UNSER, *Families of multiresolution and wavelet spaces with optimal properties*, Numer. Funct. Anal. Optim., 14 (1993), pp. 417–446.

[2] ———, *Sampling procedures in function spaces and asymptotic equivalence with Shannon's sampling theory*, Numer. Funct. Anal. Optim., 15 (1994), pp. 1–21.

[3] ———, *Families of Wavelet Transforms in Connection with Shannon's Sampling Theory and the Gabor Transform*, Wavelets- A Tutorial in Theory and Applications, 2 (1992), pp. 509–528.

[4] A. ALDROUBI, M. UNSER, AND M. EDEN, *Cardinal spline filters: stability and convergence to the ideal sinc interpolator*, Signal Process., 28 (1992), pp. 127–138.

[5] J. J. BENEDETTO AND W. HELLER, *Irregular sampling and the theory of frames*, preprint.

[6] P. J. BURT AND E. H. ADELSON, *The Laplacian pyramid as a compact code*, IEEE Trans. Comm., COM-31 (1983), pp. 337–345.

[7] P. L. BUTZER, *A survey of the Whittaker-Shannon sampling therorem and some of its extensions*, J. Math. Res. Exposition, 3 (1983), pp. 185–212.

[8] P. L. BUTZER, W. ENGELS, S. RIES, AND R. L. STENS, *The Shannon sampling series and the reconstruction of signals in terms of linear quadratic and cubic splines*, SIAM J. Appl. Math., 46 (1986), pp. 299–323.

[9] C. K. CHUI, *Multivariate Splines*, Society for Industrial and Applied Mathematics, Philadelphia, PA, 1988.

[10] C. K. CHUI AND J. Z. WANG, *A cardinal spline approach to wavelets*, Proc. Amer. Math. Soc., 113 (1991), pp. 785–793.

[11] A. COHEN, I. DAUBECHIES, AND J. C. FEAUVEAU, *Biorthogonal bases of compactly supported wavelets*, Comm. Pure Appl. Math., 45 (1992), pp. 485–560.

[12] R. R. COIFMAN, Y. MEYER, S. QUAKE, AND M. V. WICKERHAUSER, *Signal processing and compression with wave packets*, Proceedings of the Conference on Wavelets, 1989.

[13] I. DAUBECHIES, *Orthonormal bases of compactly supported wavelets*, Comm. Pure Appl. Math., 41 (1988), pp. 909–996.

[14] C. DE BOOR, *A Practical Guide to Splines*, Springer-Verlag, New York, 1978.

[15] C. DE BOOR, K. HÖLLIG, AND S. RIEMENSCHNEIDER, *Bivariate cardinal interpolation by splines on a three-direction mesh*, Illinois J. Math., 29 (1985), pp. 533–566.

[16] R. A. DEVORE, B. JAWERTH, AND B. J. LUCIER, *Image compression through wavelet transform coding*, IEEE Trans. Inform. Theory, 38 (1992), pp. 719–746.

[17] H. G. FEICHTINGER AND K. GRÖCHENIG, *Multidimensional irregular sampling of band-limited functions in L_p spaces*, ISNM 90 Oberwolfach, (1989), pp. 135–142.

[18] G. G. GILBERT, *A sampling theorem for wavelet subspaces*, IEEE Trans. Information Theory, 38 (1992), pp. 881–884.

[19] W. HACKBUSH, *Multi-Grid Methods and Applications*, Springer-Verlag, New York, 1985.

[20] J. R. HIGGINS, *Five short stories about the cardinal series*, Bull. Amer. Math. Soc., 121 (1985), pp. 45–89.

[21] H. S. HOU AND H. C. ANDREWS, *Cubic splines for image interpolation and digital filtering*, IEEE Trans. Acoust. Speech Signal Process., ASSP-26 (1978), pp. 508–517.

[22] R. HUMMEL, *Sampling for spline reconstruction*, SIAM J. Appl. Math., 43 (1983), pp. 278–288.

[23] A. K. JAIN, *Fundamentals of digital, image processing*, Prentice-Hall, Englewood Cliffs, NJ, 1989.

[24] A. J. JERRI, *The shannon sampling theorem-its various extensions and applications: A tutorial review*, Proc. IEEE, 65 (1977), pp. 1565–1596.

[25] P. G. LEMARIÉ, *Ondelettes Φ localisation exponentielles*, J. Math. Pures Appl., 67 (1988), pp. 227–236.

[26] S. G. MALLAT, *Multiresolution approximations and wavelet orthogonal bases of $L_2(\mathcal{R})$*, Trans. Amer. Math. Soc., 315 (1989), pp. 69–87.

[27] ———, *A theory of multiresolution signal decomposition: the wavelet representation*, IEEE Trans. Pattern Anal. Machine Intell., PAMI-11 (1989), pp. 674–693.

[28] M. J. MARSDEN, F. B. RICHARDS, AND S. D. RIEMENSCHNEIDER, *Cardinal spline interpolation operators on l_p data*, Indiana Univ. Math. J., 24 (1975), pp. 677–689.

[29] Y. MEYER, *Ondelettes, functions splines, et analyses graduees*, Univ. of Toronto, 1986.

[30] ———, *Ondelettes*, Hermann, Editeurs des Sciences et des Arts, Paris, 1990.

[31] M. Z. NASHED AND G. G. WALTER, *General sampling theorems for functions in reproducing kernel Hilbert spaces*, Math. Control Signals Systems, 4 (1991), pp. 373–412.

[32] P. M. PRENTER, *Splines and variational methods*, John Wiley, New York, 1975.

[33] O. RIOUL, *A discrete-time multiresolution theory*, IEEE Trans. Signal Processing, 41 (1993), pp. 2591–2606.

[34] I. J. SCHOENBERG, *Contribution to the problem of approximation of equidistant data by analytic functions*, Quart. Appl. Math., 4 (1946), pp. 45–99, 112–141.

[35] ———, *Notes on spline functions III: on the convergence of the interpolating cardinal splines as their degree tends to infinity*, Israel J. Math., 16 (1973), pp. 87–92.

[36] D. TERZOPOULOS, *Image analysis using multigrid relaxation methods*, IEEE Trans. Pattern Anal. Mach. Intell., 8 (1986), pp. 129–139.

[37] K. TORAICHI, S. YANG, M. KAMADA, AND R. MORI, *Two-dimensional spline interpolation for image reconstruction*, Pattern Recognition, 21 (1988), pp. 275–284.

[38] M. UNSER, A. ALDROUBI, AND M. EDEN, *Fast B-spline transforms for continuous image representation and interpolation*, IEEE Trans. Pattern Anal. Machine Intell., 13 (1991), pp. 277–285.

[39] ———, *Polynomial spline signal approximations: filter design and asymptotic equivalence with Shannon's sampling theorem*, IEEE Trans. Inform. Theory, 38 (1991), pp. 95–103.

[40] ———, *B-spline signal processing. Part I: Theory*, IEEE Trans. Signal Processing, 41 (1993), pp. 821–834.

[41] ———, *B-spline signal processing. Part II: Efficient design and applications*, IEEE Trans. Signal Processing, 41 (1993), pp. 834–848.

[42] M. VETTERLI, *Multi-dimensional sub-band coding: some theory and algorithms*, Signal Process., 6 (1984), pp. 97–112.

[43] M. VETTERLI AND C. HERLEY, *Wavelets and filter banks*, IEEE Trans. Signal Processing, 40 (1992), pp. 2207–2231.

[44] J. M. WHITTAKER, *Interpolation Function Theory*, Cambridge Tracts in Mathematics and Mathematical Physics, Cambridge University Press, Cambridge, UK, 1935.

[45] A. ZAYED, G. HINSEN, AND P. BUTZER, *On Lagrange interpolation and Kramer-type sampling theorems associated with Sturm-Liouville problems*, SIAM J. Appl. Math., 50 (1990), pp. 893–909.

[46] A. I. ZAYED, *On Kramer's Sampling Theorem associated with general Sturm-Liouville problems and Lagrange interpolation*, SIAM J. Appl. Math., 51 (1991), pp. 575–604.